Equilibrium, kinetic and thermodynamic studies on the removal of U(VI) by low cost agricultural waste

Abida Kausar[a]*, Haq Nawaz Bhatti[a] and Gillian MacKinnon[b]

[a] Department of Chemistry & Biochemistry, University of Agriculture, Faisalabad-38040, Pakistan. haq_nawaz@uaf.edu.pk

[b] Scottish Universities Environmental Research Centre, East Kilbride, Scotland, U.K. Gillian.MacKinnon@glasgow.ac.uk

*Email: abida.kauser@hotmail.com; Tel: +92-41-9200161-69/3319

Fax#: +92-41-9200764

Abstract

In this research, biosorption efficiency of different agro-wastes were evaluated with rice husk showing maximum biosorption capacity among the selected biosorbents. Optimization of native, SDS-treated and immobilized rice husk adsorption parameters including pH, biosorbent amount, contact time, initial U(VI) concentration and temperature for maximum U(VI) removal was investigated. Maximum biosorption capacity for native (29.56 mg g^{-1}) and immobilized biomass (17.59 mg g^{-1}) was observed at pH 4 while SDS-treated biomass showed maximum removal (28.08 mg g^{-1}) at pH 5. The Langmuir sorption isotherm model correlated best with the U(IV) biosorption equilibrium data for the 10-100 mg L^{-1} concentration range. The kinetics of the reaction followed pseudo-second order kinetic model. Thermodynamic parameters like free energy ($\Delta G°$) and enthalpy ($\Delta H°$) confirmed the spontaneous and exothermic nature of the process. Experiments to determine the regeneration capacity of the selected biosorbents and the effect of competing metal ions on biosorption capacity were also conducted. The biomass was characterised using scanning electron microscopy, surface area analysis, Fourier transformed infra-red spectroscopy and thermal gravimetric analysis. The study proved that rice husk has potential to treat uranium in wastewater.

Key words: Uranium; Biosorption; Agro-wastes; Immobilization; Desorption; Kinetics

1. Introduction

Considerable amounts of Uranium (U) have found their way into the environment through various nuclear and industrial activities, posing a threat not only to surface and groundwater but also public health [1]. The United States Environment Protection Agency set a maximum acceptable level of 30 μg L^{-1} and the World Health Organisation strictly recommends a maximum level of 2 μg L^{-1} for U [2]. Hence, the removal of U from wastewater has considerable importance. Conventional treatment techniques for the remediation of heavy metals including U, such as ion-exchange, reverse osmosis, precipitation, flocculation, electrochemical treatment, solvent extraction, adsorption on activated carbon and membrane related processes are often expensive, inefficient and produce toxic chemical sludge resulting in disposal problems [3-5]. It is therefore necessary to find suitable alternative technologies which are affordable, efficient and can complement or replace the existing methods. Biosorption is one of the possible innovative techniques involved in the remediation of heavy metals and radionuclides from wastewaters and the subsurface environment [3,6]. Biosorption involves the accumulation of metals ions by biological materials either by metabolically mediated methods or by purely physico-chemical means. Compared with conventional treatment methods, biosorption is seen as a low cost, energy-saving alternative, which has high efficiency and selectivity for absorbing metals in low concentrations and operates over broad ranges of pH and temperature. In many developing countries, the low-cost, high sorption capacity and easy regeneration of agricultural biowastes has focused attention on their use for the remediation of heavy metals from wastewater. Biosorbents including citrus waste [3], bark [7], tea waste [8], pine sawdust [9], wood powder, wheat straw [10] and activated carbon prepared from olive stones [11] have shown potential for U biosorption.

The objective of the present research was to explore and compare the biosorption efficiency of selected agricultural biowastes (rice husk, cotton sticks, peanut shell, bagasse, rice bran and wheat bran) from Pakistan for U removal from aqueous solutions. After initial screening, the most successful biosorbent (rice husk, RH) was chemically and physically treated to modify its surface characteristics which in turn, changed its biosorbent capacity. The modified RH forms (SDS-treated and immobilized) which showed increased biosorption capacity were then used to optimize the biosorption process for maximum removal of U. Although biosorptive uptake of several heavy metals on biowastes is well documented, radionuclide sorption is less well studied and to our knowledge, the use of RH for U removal is not reported in the literature. Equilibrium, kinetic and thermodynamic data are also presented.

2. Material and Methods

2.1. Collection and preparation of biosorbent

Selected agricultural wastes (rice husk, cotton sticks, peanut shell, bagasse, rice bran and wheat bran) were collected from agricultural fields and industries. Selected biowastes were extensively washed with tap water and then three times with deionized water to remove water soluble surface contaminants. After washing, biowastes were air dried at ambient temperature then finely ground (blender) and sieved to obtain a homogeneous material of uniform size (300 μm). The prepared biosorbent material was stored in air tight jars until further use.

2.2. Chemicals

All chemicals used were of analytical grade and purchased from Sigma-Aldrich Chemical Co, USA. A 1000 mg L^{-1} U(VI) stock solution was prepared by dissolving $UO_2(NO_3)_2.6H_2O$ salt in deionised water (pH 7, conductance 4 µS cm^{-1}). Working standards of desired concentration were prepared by diluting the stock solution.

2.3. Initial screening of biosorbents

Screening was carried out by adding 0.1 g of each biosorbent in 250 mL Erlenmeyer flasks containing 50 mL of 100 mg L^{-1} U(VI) solution of pH 4. Solutions were shaken for 2 h at 125 rpm and then filtered (Whatman No 42 filter paper). The filtrate was analysed for U(VI) concentration by the colorimetric method described in Section 2.4.

2.4. Analytical determination of U(VI) concentration

Quantitative analysis of the aqueous phase U(VI) concentration was carried out using the colorimetric method of Bhatti *et al*., 1991 [12]. Briefly, 0.5 mL of sample solution was mixed with 1 mL of 2.5% DTPA complexing solution and 0.5 mL Arsenazo-III in a 25 mL volumetric flask. The volume was then made up to the mark with deionised water (adjusted with 1M HCL to pH 2) and the solution allowed to develop for 3-4 minutes. The resultant pink-violet coloration of the U complex was measured at 655 nm against the corresponding blank and U concentration determined from calibrations standards prepared using the same method.

2.5. Physical and chemical pre-treatments of RH biosorbent

1.0 g sub-samples of RH biosorbent were chemically treated by shaking with 100 mL of either 5 % HCl, HNO_3, EDTA, NaOH, SDS, CTAB or NH_4OH for 2 h. Each sample was then extensively washed with deionised water and filtered (Whatman No 42 filter paper). Sub-samples of RH biosorbent were also physically modified by autoclaving (1.0 g of biosorbent/100 mL of water for 15 min) and boiling (1.0 g of biosorbent /100mL of water for 10 min). Finally, all chemically and physically treated RH samples were oven dried at 30°C, ground with a mortar and pestle and kept in air tight jars until further use.

2.6. Immobilization of RH biosorbent

Immobilization of the RH biosorbent was carried out using the method of Safa *et al*., 2011 [13]. Briefly, 1.0 g of sodium–alginate was dissolved in 100 mL of water by heating on a hotplate until boiling. Once the solution was cooled to approximately 40°C, 2 g of RH biosorbent was added and stirred until a homogeneous mixture was formed. The mixture was then added drop-wise, using a burette, into a solution of 1% $CaCl_2$ (w/v), forming uniform beads of RH immobilized Ca-alginate. The beads were kept in the 1% $CaCl_2$ (w/v) for at least one hour to allow complete curing, then washed with deionised water and stored at 4°C in deionised water until further use.

2.7. Batch biosorption studies

Batch biosorption experiments using native, SDS-treated and immobilized RH were carried out in 250 mL Erlenmeyer flasks containing 50 mL of known concentrations of U(VI) solution and amount of biosorbent with a constant shaking speed of 125 rpm for a defined

time period. To optimise the conditions for maximum U(VI) removal, different sorption affecting parameters were investigated including pH (the pH of each solution was adjusted with 1M HCl or 1M NaOH providing a range from 2-9), biosorbent amount (0.05-0.3 g), initial metal ion concentration (10-100 mgL^{-1}), contact time (5-740 min) and temperature (30–60°C). After shaking, the solution was filtered and the U(VI) concentration determined .

The biosorption equilibrium of uranium per unit biomass (mg of U g^{-1}) dry weight of the RH was calculated using the formula:

$$q_e = (C_o - C_e)\, V/W$$

Where C_o and C_e are the initial and final concentrations of U(VI) in solution (mg L^{-1}), V is volume of U(VI) solution of desired concentration per liter and W is the dry weight of RH added (g).

2.8. Effect of competing cations and anions

In order to investigate the effect of different background electrolytes on U(VI) adsorption by native, SDS-treated and immobilized RH, stock solutions of the cations (Ni^{2+}, Co^{2+}, Pb^{2+}, Mn^{2+}, Cd^{2+}, Cu^{2+}, Zn^{2+}) and anions (NO_3^{-1}, Cl^{-1}, SO_4^{2-}, PO_4^{3-}) were prepared. For this experiment, 0.05 g of biosorbent, 50 mL of 50 mg L^{-1} U(VI) solution and 25 mg $L^{-1}$of interfering ion were added to separate 250 mL Erlenmeyer flasks at pH 4 (native, immobilized RH) and pH 5 (SDS-treated RH) and the flasks agitated at 125 rpm for 320 mins (equilibrium time) at 30°C.

2.9. Desorption Studies

Desorption studies to regenerate the native RH biosorbent were conducted using EDTA, H_2SO_4, HCl, NaOH and $MgSO_4$, to compare their ability to elute adsorbed U(VI) ions. To regenerate the biosorbent, U(VI) was adsorbed under optimised conditions and the metal loaded biosorbent dried in an oven at 40°C for 24 h. The loaded biosorbent was then desorbed in 100 mL of 0.1 M solution of each selected eluting agent, by shaking for one hour at 125 rpm. The percentage of U desorbed from the biosorbent was calculated by the formula:

$$\% \, Desorption = \left[\frac{q_{des}}{q_{ads}}\right] * 100$$

And

$$q_{des} = C_{des} \, {}^{V}/_{W}$$

$q_{(des)}$ is eluted metal content (mg g^{-1}) and C_{des} is metal concentration in eluent solution mg $L^{-1.}$

The most effective eluting agent was then studied at different concentrations to further investigate its desorbing efficiency.

2.10. Biosorbent characterisation

Rice husk was physically and chemically characterised by scanning electron microscopy (SEM), Fourier transformed infra-red spectroscopy (FTIR) and thermogravimetric analysis (TGA). The specific surface area of RH was determined using a surface area analyzer (NOVA 2200e Quanta Chrome, USA) by Brunauer, Emmett and Teller (BET) and Barrett-Joyner-Halenda (BJH) methods using nitrogen as a standard. Untreated and U(VI) loaded rice

husk was coated, under vacuum, with a thin layer of gold and examined by SEM (JEOL, JSM-6400, Japan) to study surface morphology. FTIR analysis (IR Perkin Elmer 1600 spectrometer) of untreated and U(VI) loaded native, SDS-treated and immobilized RH was carried out to identify the chemical functional groups responsible for sorption of U(VI) ions. FTIR data were observed over 400-4000 cm^{-1} by preparing KBr disks containing RH biosorbent material and the resulting spectra recorded (Bio-Rad Merlin software). Thermal analysis was performed using a Perkin Elmer Diamond Series (USA) unit at a heating rate of 10°C min^{-1} (30 to 1000°C) in an inert atmosphere (N_2 100 cc (STP) min^{-1}).

2.11. Statistical analysis

Each experiment was conducted in duplicate to ensure the reproducibility of results. All data represent the mean ± standard deviation (SD) of two independent experiments.

3. Results and Discussion

3.1. Screening of biosorbents

The initial screening experiment was carried out to select the biosorbent showing the best potential for U(VI) uptake. Biosorption capacity of RH, cotton sticks, peanut shell, bagasse, rice bran and wheat bran were 26.84, 23.73, 23.71, 22.52, 21.78 and 21.70 mg g^{-1} respectively. It is clear from the obtained results that all biosorbents tested possessed good biosorption capacity for U(VI) but RH showed the highest biosorption capacity.

3.2. Effect of pre-treatments

Metal affinity to biomass can be modified by pre-treating the biomass with any base**,** acid or surfactant. The biosorption capacity (q) values of untreated (native), physically and chemically modified RH were in the following order: SDS (26.74 mg g^{-1}) > PEI (25.70 mg g^{-1}) > $MgSO_4.7H_20$ (24.81 mg g^{-1}) > boiling (24.72 mg g^{-1}) > NaOH (24.70 mg g^{-1}) > benzene (24.05 mg g^{-1}) > $CaCl_2$ (21.63 mg g^{-1}) > NH_4OH (20.78 mg g^{-1}) > HNO_3 (20.62 mg g^{-1}) = autoclave (20.62 mg g^{-1}) > $NaNO_3$ (19.73 mg g^{-1}), HCl (18.89 mg g^{-1}), H_2SO_4 (17.91 mg g^{-1}), Triton (17.64 mg g^{-1}), EDTA (16.13 mg g^{-1}), gluteraldehyde (14.83 mg g^{-1}), CTAB (14.56 mg g^{-1}) and native (13.64 mg g^{-1}). An increase in the biosorption capacity of modified RH can be attributed to increased exposure of active metal binding sites caused by chemical modifications of the cell wall components or removal of surface impurities. For example, basic pre-treatment will increase biosorption capacity by removing lipids and proteins that mask binding sites. Pre-treatment of biomass with acids may remove some mineral matter which will increase access to metal binding sites. Of greater significance however, is the introduction of oxygen surface complexes that change the surface chemistry by increasing the porosity and surface area of the original sample [13]. Surfactant pre-treatment introduces lyophobic and lyophilic groups capable of adsorbing at the biosorbent surface:solution interface. The adsorption of heavy metals onto biomass from aqueous solution can be enhanced in the presence of surfactants due to reduced surface tension and increased wetting power [14]. From all the modified treatments, SDS-treated RH showed maximum U(VI) removal and was selected for further biosorption optimization studies. This finding is complimentary to the work of Chen *et al*. [15], and Yesi *et al*. [14] who reported an increase in sorption capacity of surfactant modified silkworm exuviae and Bentonite respectively. Das et al. [16] also observed an increase in sorption capacity of two yeast species for zinc (II) removal by SDS treatment.

3.3. Effect of pH

The initial pH of the solution is critical in controlling the equilibrium loading capacity of the adsorption process. It affects the surface of the adsorbent and the chemistry of metal ion in solution which, in turn, depends upon the concentration of metal ions. The effect of pH on U(VI) sorption onto RH was studied in the pH range 2-9. Fig.1a clearly illustrates that biosorption capacity of native, SDS-treated and immobilized RH first increases with increasing pH and then decreases. Maximum biosorption capacity was observed at pH 4 for native (29.56 mg g^{-1}) and immobilized (17.59 mg g^{-1}), and pH 5 for SDS-treated (28.09 mg g^{-1}) biosorbent which is consistent with the optimum pH range for RH previously reported in the literature [3,17,18]. A further increase in pH does not favor increased biosorption capacity. This change in sorption capacity with pH can be explained by the change in uranyl ion chemistry in solution at different pHs, which also depends on U ion concentration. In acidic conditions UO_2^{2+} is the dominant species whereas at pH 4-5, monovalent uranyl species UO_2OH^+, $(UO_2)_2(OH)_2^{2+}$ [$(UO_2)_3(OH)_5^+$] are commonly found. At very low pH, the net charge on the biosorbent surface is positive which inhibits the approach of positively charged species. As pH is increased, functional groups on the biosorbent surface such as carbonyl, phosphate and amino would be available for adsorption hence maximum removal of U(VI) occurs at pH 4. U(VI) biosorption onto RH is followed by ion-exchange processes between U(VI) ions and protons introduced to the biosorbent surface of RH by acids. At very high pH, insoluble precipitates of uranium such as schoepite ($4UO_3.9H_2O$) form in solution, decreasing the uranium concentration in solution which subsequently leads to a lower biosorption capacity of RH [3].

3.4. Effect of biosorbent amount

Removal efficiency of any biomass is highly dependent upon sorbent amount as it controls the sorbate-sorbent equilibrium of the sorption system. This is due to fact that the number of available binding functional groups on the adsorbent surface is a function of adsorbent amount. The effect of biosorbent amount on U(VI) biosorption was studied in range 0.05-0.3 g/50 mL of 50 mg L^{-1} U(VI) solution and the results are illustrated in Fig.1b. Results indicated that a maximum biosorption capacity of 29.6, 31.6 and 27.8 mg g^{-1} was obtained for native, SDS-treated and immobilized RH respectively with 0.05 g. Further increase in biosorbent amount decreased the biosorption capacity which could be due to the fact that the increase in biomass amount caused aggregation of the biomass particles and subsequently decreased the available surface area for biosorption of U(VI) ions. [3].

3.5. Effect of contact time

The effect of contact time on the biosorption of U(VI) by native, SDS-treated and immobilized RH was investigated over the time intervals of 5 to 740 min as shown in Fig.1c. A maximum biosorption capacity value of 39.9 mg g^{-1} for native RH was obtained after 320 min and 41.0 and 31.9 mg g^{-1} was obtained for SDS-treated and immobilized RH respectively after 740 min. During the initial stages of the sorption process, adsorption rate was rapid, after which, uptake rate slowly declined and tended to attain equilibrium at 320 min. It can be hypothesized that during the initial stages of the adsorption process, the higher concentration of U(VI)) ions provide the driving force to facilitate ion diffusion from solution to the active sites of the biosorbent. As the process continues, occupation of the active sites and the decrease of the U(VI) ion concentration, leads to a decrease in uptake rate until

equilibrium is achieved [3,6]. The equilibrium time for U(VI) biosorption by RH is in accordance with the previously reported U biosorption studies on other biosorbents [6,19].

3.6. Biosorption kinetic modeling

In order to examine the diffusion mechanism involved during the adsorption process, various kinetic models were tested i.e. pseudo-first order [20], pseudo-second-order [21], intra-particle diffusion [22] and the Elovich model [23]. The applicability of these kinetic models was determined by measuring the correlation coefficients (R^2) as well as closeness of values between experimental and calculated sorption capacity values.

Pseudo-first-order kinetic model is based on the fact that the change in uranium ions concentration with respect to time is proportional to the power one. The following linear form of the pseudo-first-order model was used to study U(VI) biosorption onto RH biosorbents:.

$$\log(q_e - q_t) = \log(q_e) - \frac{q_1}{2.303} t$$

Where q_e and q_t are the amount of U(VI) adsorbed (mg g^{-1}) at equilibrium and at time t (min), respectively, and k_1 (min^{-1}) is the pseudo-first-order rate constant. Values of k_1 are calculated from the plots of $\log(q_e - q_t)$ versus t. The R^2 values obtained for native, SDS-treated and immobilized RH are presented in Table 1. These values are relatively small and the experimental q_e values do not agree with the values calculated from the linear plots suggesting the pseudo-first-order kinetic model is not well fitted to the data obtained for contact time.

The biosorption mechanism over the range of contact time is better explained by the pseudo-second-order kinetic model. This equation is shown below:

$$\frac{t}{q_t} = \frac{1}{K.q_e^2} + \left(\frac{1}{q_e}\right) t$$

Where q_e and q_t are the amount of U(VI) adsorbed on adsorbent (mg g^{-1}) at equilibrium and at time t (min), respectively, and k_2 is the pseudo-second-order rate constant (g mg^{-1} min^{-1}). Based on the experimental data of q_t and t, the equilibrium adsorption capacity (q_e) and the pseudo-second-order rate constant (k_2) can be determined from the slope and intercept of a plot of t/q_t versus t. It was found that the pseudo-second-order model provides the best fit for all three RH forms.

The Morris–Weber equation is generally applied to evaluate the intraparticle rate constant, R_{id} using the following relationship:

$$q_t = R_{id}.t^{1/2}$$

where q_t is the sorbed concentration at time t and R_{id} is the rate constant of intraparticle transport. From the slope of the linear plot q_t vs. $t^{1/2}$, the rate constant R_{id} may be calculated. This kinetic model was applied to the different sorption experimental data obtained for native, SDS-treated and immobilized forms of RH but showed very low R^2 value for all.

The Elovich kinetic model can also be used to explain the biosorption process. The equation is written as follows:

$$q_t = {}^{1}/_{\beta l_n}(\alpha\beta) + {}^{1}/_{\beta}\ln(t)$$

Where α is the initial adsorption rate (mg g^{-1} min^{-1}) and β is the desorption constant (g mg^{-1}). The values of α, β and the correlation coefficient R^2 for native, SDS-treated and immobilized RH are given in Table 1. The experimental data fit well to the Elovich kinetic model, as is evident from the R^2 values.

The applicability of both pseudo-second-order and Elovich kinetic models to the experimental data suggests chemisorption is the dominant process in controlling U(VI) uptake on RH.

3.7. Effect of initial U(VI) ion concentration

The effect of changing U(VI) ion concentration was studied in the range of 10-100 mg L^{-1} by keeping the other parameters (pH 4, biosorbent dose 0.05 g, temperature 30°C, shaking speed 125 rpm) constant. The effect of U(VI) concentration is shown in Fig.1d and illustrates the uptake capacity of native, SDS-treated and immobilized RH increases rapidly before becoming constant after a certain concentration. The initial rapid increase is due to the availability of more active sites which then become saturated. Gan Tian observed the same trend during uranium sorption using oxime-grafted ordered mesoporous carbon CMK-5 for concentrations in the range of 25-250 mg L^{-1} [24].

3.8. Isotherm modeling

The search for the best fit equation using linear regression analysis is the most commonly used technique to determine the most suitable isotherm to explain the mechanism for adsorption. The equilibrium data obtained from the U(VI) concentration on sorption capacity experiment was interpreted by different isotherms and presented in Table 2.

3.8.1. Langmuir isotherm

The Langmuir model [25] assumes that the removal of metal ions occurs on an energetically homogenous surface by monolayer sorption and there are no interactions between the adsorbate on adjacent sites.

$$\frac{C_e}{q_e} = \frac{1}{q_m} Ce + \frac{1}{K_a q_m}$$

Where q_e is the amount of U(VI) ions biosorbed on the biomass (mg g^{-1}) at equilibrium, Ce is the equilibrium concentration of U(VI) ions, q_m is the maximum biosorption capacity describing a complete monolayer adsorption (mg g^{-1}) and K_a is the adsorption equilibrium constant (L mg^{-1}) that is related to the free energy of biosorption.

The important features of the Langmuir isotherm model can be defined by the dimensionless constant separation factor R_L which is expressed by:

$$R_L = {}^{1}/_{1 + k_a C_o}$$

where C_o is the initial metal ion concentration (mg L^{-1}) and K_a is the Langmuir constant (L mg^{-1}). R_L shows the nature of the biosorption mechanism.

R_L value	**Nature of biosorption mechanism**
RL > 1	Unfavorable
RL = 1	Linear
0< RL<1	Favorable
RL = 0	Irreversible

The values of R_L obtained in the present study were in the range 0-1 (see Table 2), showing the biosorption process to be favorable for U(VI) removal for native and modified RH.

3.8.2. Freundlich model

The Freundlich isotherm [26] is based on the assumption that the biosorption process takes place by interaction of metal ions on a heterogeneous surface. There is a logarithmic decline in the energy of biosorption with the increase in the occupied binding sites.

The linear form of the Freundlich isotherm equation is:

$$\log(q_e) = \log(K_F) + {}^{1}/_{n_F} \log(C_e)$$

Where K_F is the Freundlich isotherm constant (mg g^{-1}) related to the bonding energy. K_F is defined as the distribution coefficient and suggests the amount of U(VI) sorbed on the biosorbent for unit equilibrium concentration. The value of n indicates whether the biosorption process is favorable (n >1 – 10) or not. The values of n shown in Table 2 suggest the process of U(VI) adsorption is highly favorable on RH.

3.8.3. Temkin isotherm

The Temkin isotherm model [27] suggests an equal distribution of binding energies over a number of exchange sites on the surface. The linear form of the Temkin isotherm can be written as:

$$q_e = B\ln A + B\ln C_e$$

where B is equal to RT/b with R being the universal gas constant (8.314J mol^{-1} K^{-1}) and T being the absolute temperature in Kelvin. A is the equilibrium binding constant and B corresponds to the heat of sorption. The high R^2 values for native and modified RH show good fit of the U(VI) biosorption data to the Temkin equation.

3.8.4. Flory-Huggins model

The Flory–Huggins model [28] was chosen to account for the degree of surface coverage characteristics of the sorbate on the sorbent. The isotherm is as follows:

$$\log {\theta}/{C_o} = \log K_{FH} + n_{FH}\log(1-\theta)$$

where $\theta = (1-C_f/C_0)$ is the degree of surface coverage, K_{FH} is the Flory–Huggins model equilibrium constant and n_{FH} the Flory–Huggins model exponent.

3.8.5. Dubinin–Radushkevich isotherm

Another useful equation for the analysis of isotherms of a high degree of regularity was proposed by the Dubinin–Radushkevich (D-R) isotherm [29]. They reported that the characteristic sorption curve is related to the porous structure of the sorbent.

$$lnq = lnq_m - \beta\varepsilon^2$$

The Polanyi sorption potential ε, which is the amount of energy required to pull a sorbed molecule from its sorption site to infinity may be evaluated by using relationship:

$$\varepsilon = RT\ln\left[1 + \frac{1}{C_e}\right]$$

$$E = \frac{1}{\sqrt{-2\beta}}$$

One of the best features of the D-R equation is the fact that it is temperature dependent. If the adsorption data at different temperatures are plotted as the logarithm of the amount adsorbed versus the square of potential energy, all the suitable data shall in general lie on the same curve, called the characteristic curve. The mean biosorption energy value, which is in the range of 1–8 kJ/mol and 9–16 kJ/mol, forecasts the physical biosorption and chemical biosorption or ion-exchange, respectively. The experimental values of E calculated show the ion exchange and chemisorption nature of the process.

3.8.6. Halsey Model

Halsey [30] proposed an expression for condensation of a multilayer process at a relatively large distance from the surface:

$$\log q_e = {}^{1}/_{n_H}\log K_H - {}^{1}/_{n_H}\log C_e$$

A linear plot between log q_e vs log C_e gives the values of Halsey constant n_H and K_H from the slope and intercept respectively.

3.8.7. Harkin Jurra

The Harkin-Jura [31] adsorption isotherm can be expressed as:

$$^{1}/_{q_e^2} = {}^{B}/_{A} - {}^{1}/_{A\ log\ C_e}$$

where A and B are the constants calculated from the slope and intercept of the linear plot between $1/qe^2$ and $logC_e$. The isotherm equation also accounts for multilayer adsorption and explains the existence of a heterogeneous pore distribution. The R^2 values show the fitness of the model for U(VI) removal by RH.

3.9. Effect of temperature

The effect of temperature on biosorption of U(VI) ions onto native, SDS-treated and immobilized RH is shown in Fig.1e. The effect of temperature on the biosorption process was small and the maximum biosorption capacity was obtained at 30°C. Decrease in the biosorption capacity was observed at high temperature and the effect was more pronounced in SDS-treated RH as compared to native and immobilized forms.

3.10. Thermodynamics of U(VI) sorption

Thermodynamic parameters such as standard Gibbs free energy change (ΔG°), standard enthalpy change (ΔH°) and standard entropy change (ΔS°) were estimated from the following equations:

$$l_n K_c = -\left(\Delta H^0/_R\right) 1/_T + \Delta S^0/_R$$

Where $K_c = (q/C_e)$ is the distribution coefficient (mL g^{-1})

The values of ΔH° and ΔS° are calculated from the slope and intercept of the linear variation of the plot between $\log(q/C_e)$ and 1/T.

The value of ΔG° is calculated as:

$$\Delta G^0 = \Delta H^o - T\Delta S^0$$

Thermodynamic parameters at various temperatures for native, SDS-treated and immobilized RH are presented in Table 3. The negative value of ΔH^o suggests that the process is exothermic with ΔH° values less than 40 kJ mol^{-1}, suggesting the reaction is physical in nature. The negative values of ΔG° for all three forms of RH provide evidence of the spontaneity of the reaction. The positive values of entropy change ΔS° suggest that randomness increases as the reaction proceeds and biosorption of U(VI) ions onto native, SDS-treated and immobilized RH is a favourable process.

3.11. Effect of competing cations and anions

Uranium biosorption by RH in the presence of equimolar concentrations of other cations and anions was studied. Industrial wastewater contains many other background electolytes which may interfere with the biosorption process so the biosorption process must perform effectively in the presence of these competing ions. Solutions of competing ions having the same ionic strength as those found in wastewater were prepared and the influence on the biosorption capacity of RH biosorbents was studied. The effect of ionic interaction on the

sorption process may be represented by the ratio of sorption capacity in the presence of interfering ion (q_{mix}) and without interfering ion (q_0), such that for:

$\frac{q_{mix}}{q_0}$ >1 sorption is promoted in presence of other interfering ions

$\frac{q_{mix}}{q_0}$ =1 sorption is not influenced in presence of other interfering ions

$\frac{q_{mix}}{q_0}$ < 1 sorption is suppressed in presence of other interfering ions [32]

The effect of cations and anions on the biosorption capacity of RH is reported in Table 4. Among the cations studied, no significant effect on adsorption capacity of native and SDS-treated RH was observed at low concentration (50 ppm) but at higher concentrations, these competing cations showed an inhibiting effect. In the case of the anions selected, nitrate caused the maximum interference on native and SDS-treated RH forms while sulphate and phosphate also had suppressing effects. The immobilized RH appeared not to be strongly influenced by the presence of these anions. Chloride did not seem to compete with the U(VI) ions for adsorption sites on native and SDS-treated RH but greatly suppressed adsorption on the immobilized RH.

3.12. Adsorption-desorption studies

Desorption of the adsorbed U(VI) ions as a function of fixed U(VI) concentration by different desorbing agents was studied in a batch system. Desorption efficiency of the selected chemicals was found to be at a maximum with H_2SO_4 for native and SDS-treated RH (86 %) and with EDTA for immobilized RH (92%). The selected desorbing agents efficiency decrease in following order for native, SDS-treated and immobilized RH respectively.

H_2SO_4 > HCl > EDTA >NaOH >$MgSO_4$ (native)

H_2SO_4 > HCl > EDTA >NaOH >$MgSO_4$ (SDS-treated)

EDTA > HCl > H_2SO_4>NaOH >$MgSO_4$ (immobilized)

A desorption experiment to study the effect of changing concentrations of H_2SO_4 was conducted for native and SDS-treated RH. The results indicate that the elution capacity of native and SDS-treated RH by H_2SO_4 increased from 79 to 92% and 87 to 94% respectively when the H_2SO_4 concentration was increased from 0.1M to 0.5M. The elution capacity of the immobilized RH was increased from 92% to 98% by increasing the EDTA concentration from 0.1M to 0.5M.

3.13. FTIR analysis

The presence of active functional groups responsible for U(VI) adsorption onto native RH is confirmed by FTIR (see Fig. 2a). The organic part of the RH is composed of cellulose, hemicelluloses and lignin, which contain mostly alkenes, esters, aromatics, ketones and aldehydes. The presence of OH groups on the RH is confirmed by presence of a band between 3000 and 3750 cm^{-1}. OH groups bound to methyl radicals, which are common in lignin, show a signal between 2940-2820 cm^{-1}. The peak at 1053 cm^{-1} represents the Si-O-Si linkage as part of the inorganic portion of the RH. Comparative analysis of vibrational frequencies of the functional groups of biosorbents (native RH, SDS treated and immobilized RH shown in Fig. 2.a) shows the involvement of cellulose, lignin and silica functional moieties in adsorption [33].

3.14. TGA analysis

In TGA, the lignocellulosic structure of biosorbents can be qualitatively identified from the change in weight of a sample which is recorded as a function of time or temperature. As illustrated in Fig.2b, the first stage (below 200°C) corresponded to the drying period where light volatiles, mainly water were liberated causing minimal reduction in sample weight, . The second stage of decomposition, occurring between 200 and 500°C, corresponds to a significant percentage weight loss of sample due to liberation of volatile hydrocarbons from rapid thermal decomposition of hemicelluloses, cellulose and some parts of lignin. During stage 3, a continuous weight loss was observed until the highest temperature was reached (1000°C), primarily due to the steady decomposition of the remaining heavy components mainly from lignin [34].

3.15. Surface studies of RH

Physiochemical properties of the native RH were determined and results showed that BET specific surface area, BJH total pore volume and pore diameter were 58.48 m^2/g, 0.32 cc g^{-1} and 129.14 A^0 respectively. The results obtained highlight the predominance of meso-pores (IUPAC Classification 20Å < d < 500 Å) in RH which is desirable for the adsorption of metal ions from the aqueous phase [35]. This is supported by the SEM images of the surface morphology of untreated RH, before and after loading with U(VI) ions as is illustrated in Fig.3.

4. Conclusions

The most promising biosorbents were recognised, considering criteria such as cost, biosorption effectiveness and re-use potential for U(VI) wastewater treatment. It has been shown that the biosorption of U(VI) on native, SDS-treated an immobilized RH is influenced by several factors, such as pH, biosorbent dose, initial U(VI) concentration, contact time and temperature. The detailed equilibrium and kinetic study showed that the Langmuir isotherm and pseudo-second-order equations were best fitted to the experimental data. FTIR, SEM, BET and TGA demonstrated RH surface characteristics responsible for U(VI) removal. The effect of competing ions showed that the RH biosorbents can be successfully applied in the presence of low concentrations of these ions. Finally we can say, after comparison of the present work with previously reported synthetic and natural sorbents (Table 5), that RH in native and modified forms provides a potential alternative for the purification treatment of U(VI) containing wastewaters because of its excellent performance for removal and recovery.

Acknowledgments

The authors are grateful for the financial support of this project by Higher Education Commission (HEC) of Pakistan under the Indigenous Ph.D. Fellowship Program.

References

[1] R. O. Abdel Rahman, H. A. Ibrahium and Y-T Hung, Water. 3 (2011) 565.

[2] N. Saifuddin, and S. Dinara, Adv. in Nat. Appl. Sci. 6 (2012) 249.

[3] N. Saleem and H. N.Bhatti, Bioresources. 6 (2011) 2522.

[4] Z-j. Yi and J. Yao, J. Radioanal. Nucl. Chem. 293 (2012) 907.

[5] S. Aytas, D.A. Turkozu and C.Gok, Desalination. 280 (2011) 354.

[6] C. Panga, Y-H Liua, X-H Caob, M. Li, G-L Huangb, R. Huab, C-X Wangb, Y-T Liub, and X-F. Anb, Chem. Eng. J. 170 (2011) 1.

[7] L. Jauberty, V.Gloaguen, C. Astier, P. Krausz, V. Delpech, A. Berland, V. Granger, Decossas, Z-J. Yi and J. Y. J. Radioanal. Nucl. Chem. 29 (2012) 907.

[8] D-X Ding, X-T Liu, N. Hu, G-Y. Li, Y-D. Wang. J. Radioanal. Nucl. Chem. 293 (2012) 735.

[9] W. Zou and l. Zhao, J. Radioanal. Nucl. Chem. 291 (2012) 585.

[10] S. B. A. Lakzian, S.J. A. M. F.Rahimi, A. Halajnia, J. Radioanal. Nucl. Chem. 283 (2010) 289.

[11] C. Kütahyalı and M. Eral. J. Nucl. Mat. 396 (2010) 251.

[12] T. M. Bhatti, A.M. .Amin, K. A. Malik and A. M. Khalid. J.Chem.Tech.Biotechnol. 52 (1991) 33.

[13] Y. Safa, H.N. Bhatti, I.A.Bhatti, M. Asgher, J. Chem. Eng. 89 (2011) 1565.

[14] Yesi, F. P. Sisnandy. Y-H Ju, F. E.Soetaredjo, S. Ismadji, Adsorpt. Sci. Technol. 28 (2010) 847.

[15] H. Chen, J. Zhao, J.Y. Wu and G.L. Dai, J. Hazarad. Mat, 192 (2011) 246.

[16] D. Das, G. Basak, V. Lakshmi and N. Das. Biochem. Eng. J. 64 (2012) 30.

[17] S. Aytas, D. A. Turkozu and C. Gok. Desalination. 280 (2011) 354

[18] C. Zhou, Z. Shang, Z. Liu, G. Huang and A.A Adesina. J. Colloid Interface Sci. 366 (2012) 165.

[19] C. Pang, Y. Liu, X. Cao, R. Hua and C. C.Li. J. Radioanal. Nucl. Chem. 286 (2010) 185.

[20] S. Lagergren, Handlingar, 24 (1898) 1.

[21] Y.S. Ho and G. Mckay, Process. Biochem. 34 (1999*)* 451.

[22] W.J. Morris and J.C. Weber, J. Saint. Enging. Division, ASCE, 89 (1963) 31.

[23] M.J.D. Low. Chem. Reviews. 60 (1960) 267.

[24] G. Tian, J. Geng, Y. Jin, C. Wang, S. Li, Z. Chen, H. Wang, Y. Zhao and S. Li. J. Hazard. Mater. 190 (2011) 442.

[25] I. Langmuir, J. Am. Chem. Soc. 38 (1916) 2221.

[26] H.M.F. Freundlich. J. Phys. Chem. 57 (1906) 385.

[27] M. J. Temkin and V. Pyzhev. cta. Physiochim. USSR, 12 (1940) 217.

[28] M. Horsfall and A.I. Spiff. 52 (2005) 174.

[29] M.M. Dubinin and L.V. Radushkevich, Chem. Zentr. 1 (1947) 875.

[30] G. Halsey, J. Chem. Phys.16 (1948) 931.

[31] W.D. Harkins and E.J. Jura. J. Chem. Phys. 12 (1944) 112.

[32] F. V. Pereira, L. V.A. Gurgel and L.F. Gil. J. Hazard Mat. 176 (2010) 856.

[33] W. Nakbanpote, B. A. Goodmanb, P. Thiravetyanc. Colloids Sufaces A: Physicochem Eng Aspects. 304 (2007) 7.

[34] M. Ghorbania and H. Eisazadehb. Synthetic Metals. 162 (2012)1429.

[35] V. M. Srivastava, I. D. Mall, I. M. Mishra. J. Hazard Mater. 134 (2006) 257.

[36] D.M.G. Saad, E.M.Cukrowska and H.Tutu. Water. Sci Technol. 66 (2012) 122.

[37] C. Özeroğlu and N. Metin. J. Radioanal. Nucl. Chem. 291 (2012) 923.

[38] S. Kumar, V.A . Loganathan, R.B. Gupta and M.O. Barnett. J. Environ. Manage. 92 (2011) 2504.

[39] M. Sprynskyya, T. Kowalkowskia, H. Tutub, E. M. Cukrowskab and B. Buszewski. Chem. Eng. J. 171 (2011) 1185.

[40] M. Sprynskyy, I. Kovalchuka and B. Buszewskia. J. Hazard Mater. 18 (2010) 700.

[41] T.S. Anirudhan and S.S. Sreekumari. Colloids Surfaces A: Physicochem Eng Aspects. 361 (2010) 180.

[42] S. Ayata, S.Aydinci, M. Merdivan, G. Binzet and N.Kulcu. J. Radioanal. Nucl. Chem. 285 (2010) 525.

Figure Captions.

Fig. 1. (a) Effect of pH on biosorption of U(VI) (b) Effect of sorbent amount on biosorption of U(VI). (c) Effect of time on biosorption of U(VI). (d) Effect of initial metal ion concentration on biosorption of U(VI). (e) Effect of temperature on biosorption of U(VI). Mean values given ± SD, n = 2.

Fig. 2. (a). FT-IR spectra of native rice husk and U(VI) loaded rice husk and comparative analysis of vibrational frequencies of the functional groups of rice husk (native, SDS-treated and immobilised). (b)Effect of temperature on native rice husk, scan of heating from 30°C to 1000°C at 10°C/min in N_2 atmosphere; initial sample weight 9.102 mg.

Fig. 3. Scanning electron micrographs of native rice husk unloaded (a) (×500), (b) (×1000) and Uranium loaded rice husk (c) (×500), (d) (×1000).

Fig. 1.

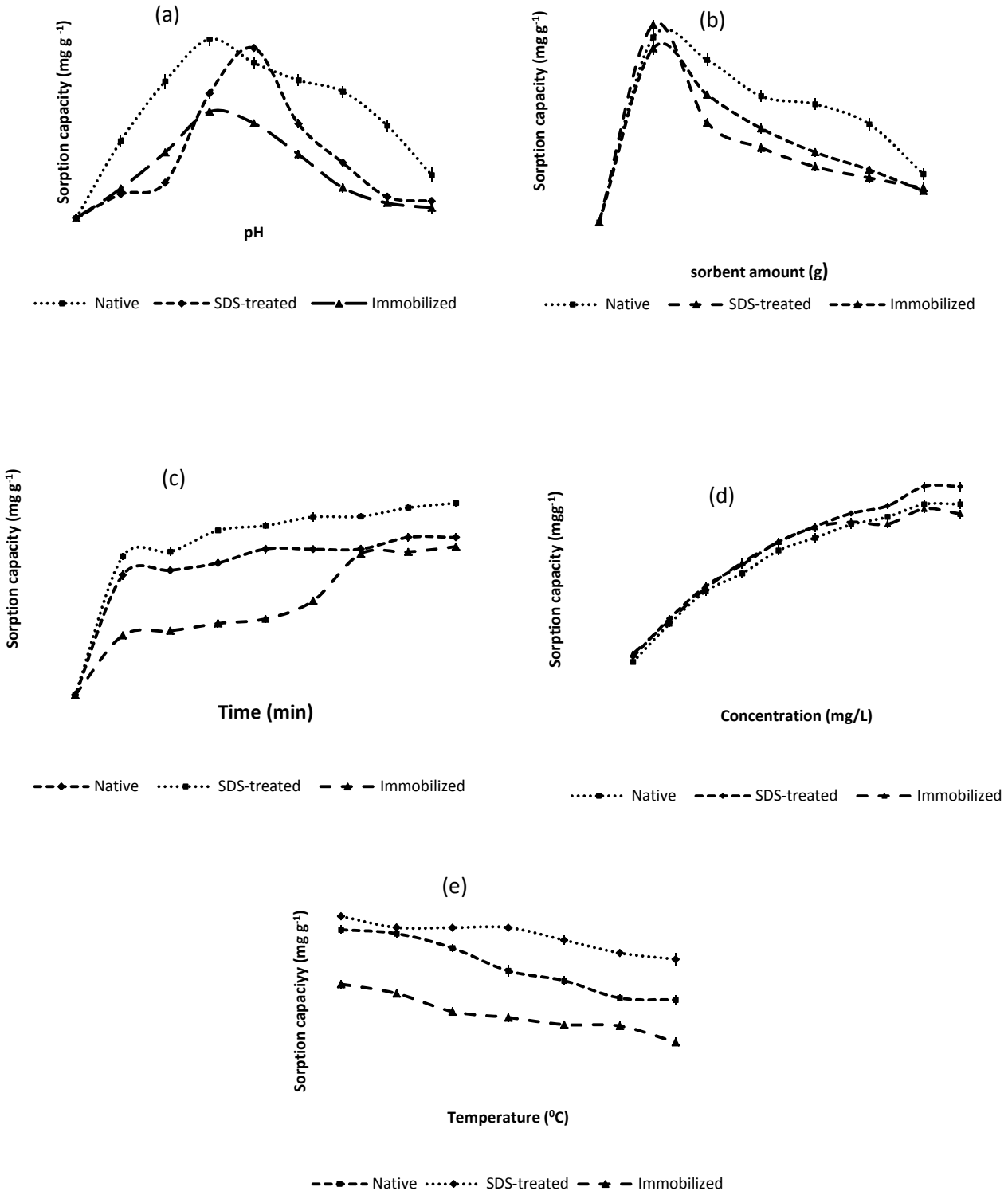
(a)
Sorption capacity (mg g-1)
pH
Native
SDS-treated
Immobilized
(b)
Sorption capacity (mg g-1)
sorbent amount (g)
Native
SDS-treated
Immobilized
(c)
Sorption capacity (mg g-1)
Time (min)
Native
SDS-treated
Immobilized
(d)
Sorption capacity (mgg-1)
Concentration (mg/L)
Native
SDS-treated
Immobilized
(e)
Sorption capaciyy (mg g-1)
Temperature (0C)
Native
SDS-treated
Immobilized

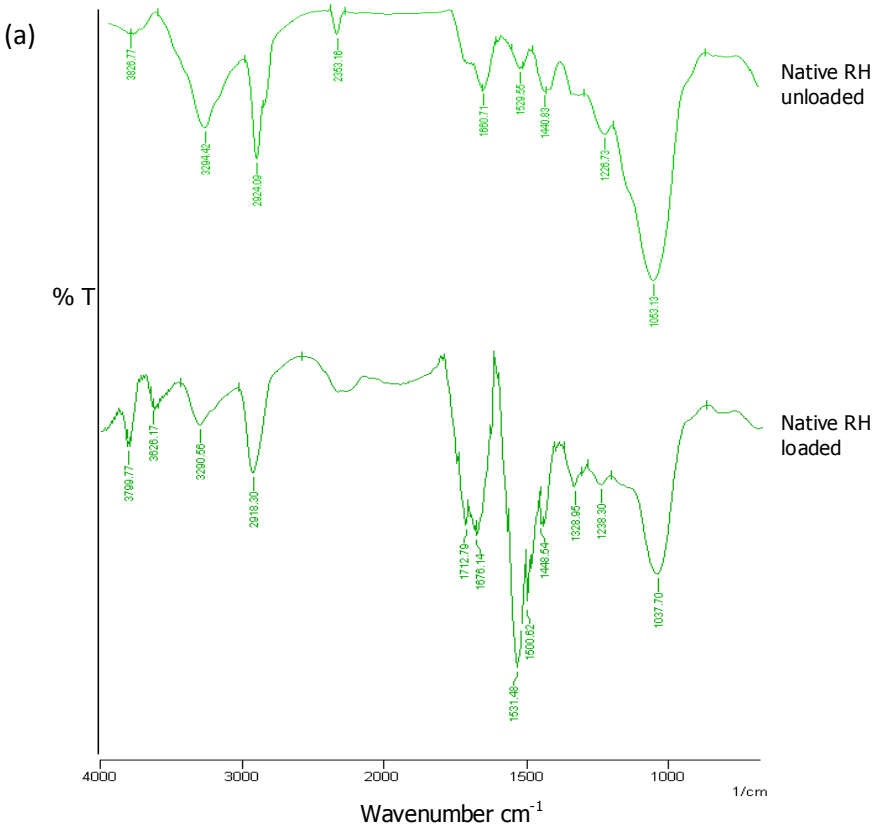

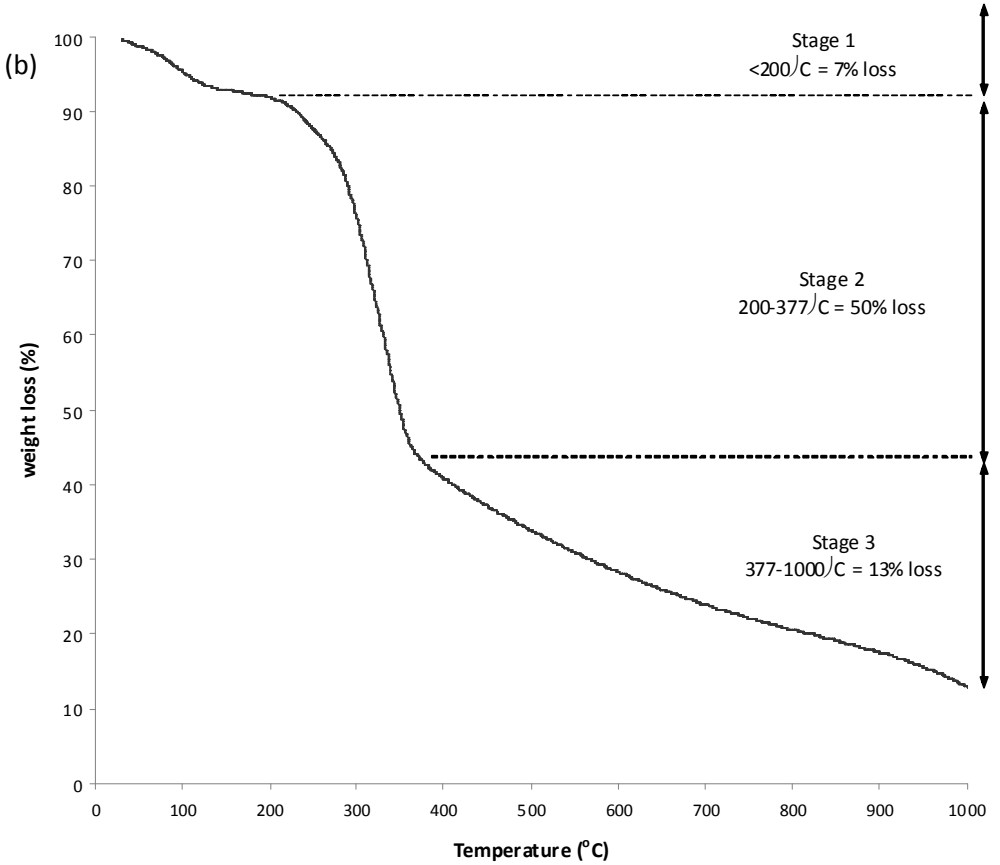

unloaded RH	loaded RH	SDS treated loaded RH	Immobilized loaded RH
3826.77 cm^{-1} (Si-OH)	Absent	3761.19	3761.19
3294.42 (O-H stretching of hydroxyl cellulose)	3290.56	3442.94	Absent
2924.09 (OH bound to $-CH_3$ of lignin)	2918.30	2929.87	2924.09
1529.55 (Aromatic C=C stretching Lignin/phenolic backbone)	1531.4	1585.49	1587.42
1053.13 (Si-O-Si)	1037.70	1072.42	1064.71

Fig. 2.

Fig.3.

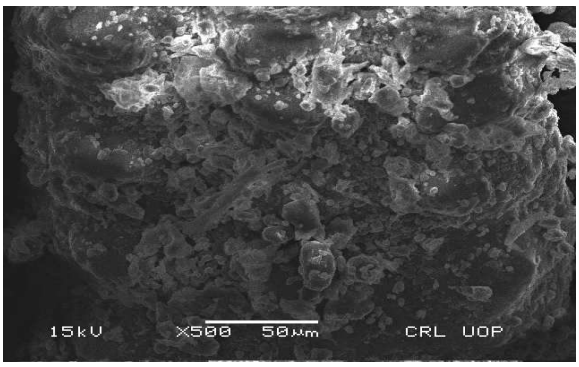
15kV X500 50µm CRL UOP

(a)

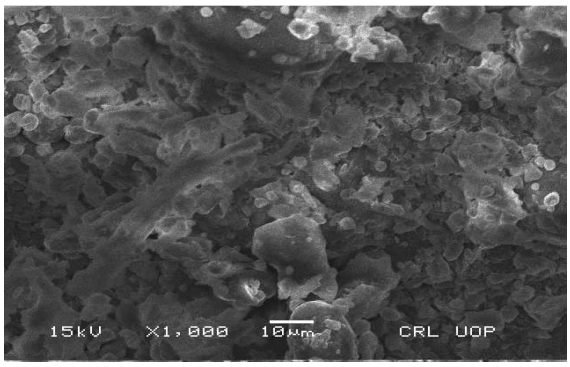
15kV X1,000 10µm CRL UOP

(b)

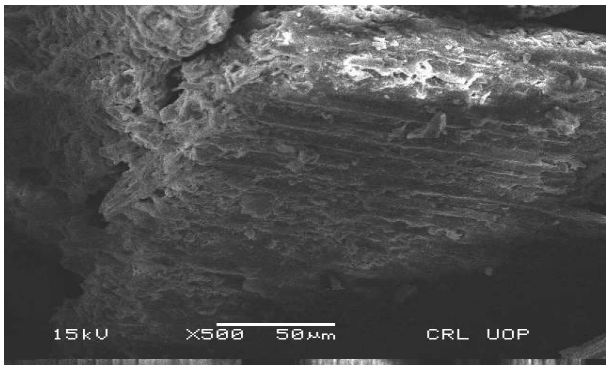
15kV X500 50µm CRL UOP

(c)

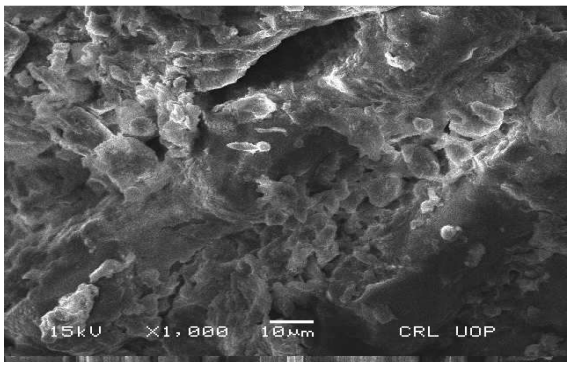
15kV X1,000 10µm CRL UOP

(d)

Table 1. Comparative study of kinetic parameters for the biosorption of U(VI) onto rice husk biosorbents.

Kinetic models	Native	SDS-treated	Immobilized
Pseudo-first order			
K1(L min^{-1})	0.0000690	0.00138	0.00110
q_e experimental (mg/g)	33.9	42.3	30.9
q_e calculated(mg/g)	4.04	10.4	5.24
R^2	0.582	0.562	0.670
Pseudo-second order			
K_2(g/mg min)	0.0069	0.0064	0.000924
q_e experimental (mg/g)	33.9	42.3	30.9
q_e calculated (mg/g)	34.1	40.5	32.8
R^2	0.999	0.999	0.997
Intraparticle diffusion model	0.0176	0.0211	0.0518
Kpi (mg/g$min^{1/2}$)	28.9	34.4	17.0
Ci	0.528	0.443	0.634
R^2			
Elovich			
α(mg$g^{-1}min^{-1}$)	1.85 x10^{11}	0.771	1.60
β(gmg^{-1})	0.587	0.454	0.220
R^2	0.923	0.902	0.897

Table 2. Comparative study of equilibrium isotherm parameters for the biosorption of U(VI) onto rice husk biosorbents.

Isothermal model	Native	SDS-treated	Immobilized
Langmuir			
q_m(mg/g)	45.2	47.2	40.0
K_a(L/mg)	0.0990	0.129	0.212
R_L	0.101	0.0790	0.0498
R^2	0.997	0.991	0.995
Freundlich			
q_m(mg/g)	36.2	40.9	35.3
K_F	7.19	9.59	1.18
n	2.25	2.58	3.32
R^2	0.944	0.982	0.970
Temkin	1.19	2.17	4.26
A (l/g)	271	310	367
B	35.7	36.7	20.8
q_m(mg/g)	0.997	0.988	0.953
R^2			
Flory-Huggins			
$n_{(FH)}$	3.49	1.80	1.30
$k_{(FH)}$	1.2×10^{-3}	1.8×10^{-3}	3.0×10^{-3}
R^2	0.988	0.986	0.908
Harkin jurra			
A	125	172	212
B	1.60	1.61	1.66
R^2	0.657	0.752	0.857
Halsey			
q_{max} (mg/g)	36.3	40.9	35.4
K_H	0.0116	2.95	2.74
n_H	2.26	2.58	3.56
R^2	0.943	0.982	0.969
D-R isotherm			
B mol^2/kJ^2	0.001	0.003	0.0001
q_m (mg/g)	31.7	32.6	30.1
E (kJ/mol)	22.4	12.9	70.9
R^2	0.853	0.750	0.676

Table 3. Thermodynamic parameters for biosorption of 50 mg L^{-1} U (VI) onto rice husk bisorbents as a function of temperature (initial pH 4 for native and immobilized, pH 5 for SDS-treated, shaking time 320 min).

Temperature (C^o)	Native			SDS-treated			Immobilized		
	ΔG°	**ΔH°**	**ΔS°**	**ΔG°**	**ΔH°**	**ΔS°**	**ΔG°**	**ΔH°**	**ΔS°**
30	-37.57			-30.89			-21.94		
35	-38.19			-31.39			-22.29		
40	-38.81	-113.3	123.6	-31.91	-86.95	101.7	-22.66	-70.18	72.16
45	-39.43			-32.42			-23.02		
50	-40.05			-32.92			-23.38		
55	-40.66			-33.43			-23.74		
60	-41.28			-33.94			-24.10		

* ΔG^o= kJ mol^{-1}; ΔH^o= kJ mol^{-1}; ΔS^o= J mol^{-1} K^{-1}

Table 4. Comparison of the effect of different interfering cations and anions on 50 mg L^{-1} U(VI) biosorption onto rice husk biosrobents (initial pH 4 for native and immobilized, pH 5 for SDS-treated, shaking time 320 min).

Cations	$\frac{q_{mix}}{q_0}$ **Native**			$\frac{q_{mix}}{q_0}$ **SDS-Treated**			$\frac{q_{mix}}{q_0}$ **Immobilized**		
	50 ppm	75 ppm	100 ppm	50 ppm	75 ppm	100 ppm	50 ppm	75 ppm	100 ppm
Ni^{+2}	0.98	0.62	0.66	0.85	0.62	0.66	0.72	0.28	0.06
Pb^{+2}	0.97	0.84	0.66	0.84	0.68	0.43	0.88	0.24	0.02
Co^{+2}	0.97	0.32	0.13	0.84	0.64	0.43	1.11	0.50	0.27
Mn^{+2}	0.96	0.89	0.79	0.85	0.75	0.52	1.54	0.78	0.77
Cd^{+2}	0.96	0.64	0.61	0.75	0.62	0.43	0.82	0.63	0.53
Cu^{+2}	0.96	0.69	0.58	0.83	0.75	0.53	0.39	0.24	0.17
Zn^{+2}	0.96	0.97	0.27	0.79	0.75	0.49	0.98	0.66	0.34

Anions	$\frac{q_{mix}}{q_0}$ **Native**	$\frac{q_{mix}}{q_0}$ **SDS-Treated**	$\frac{q_{mix}}{q_0}$ **Immobilized**
	0.1M	0.1M	0.1M
NO_3^{-1}	0.68	0.89	0.99
Cl^{-1}	0.91	0.94	0.04
SO_4^{2-}	0.79	1.00	1.02
PO_4^{3-}	0.88	0.94	0.94

Table 5. Comparison of sorption capacities of different adsorbents for U(VI) removal from wastewater

Adsorbents	Adsorption capacity (initial U(VI) concentration)	Reference
Fe_3O_4@SiO_2 composite	52 mg g^{-1} (20-200 mg L^{-1})	36
poly(methacrylic acid)-grafted chitosan/bentonite (CTS-g-PMAA/Bent) composite	117 mg g^{-1} (100-250 mg L^{-1})	37
lignocellulosic biochar	42 mg g^{-1} (100 mg L^{-1})	38
CMK-5 (Oxime-CMK-5)	65.2 mg g^{-1} (25–300 mg L^{-1})	24
Penicillium citrinum	127 mg g^{-1} (30-80 µg mL^{-1})	6
Talc	41.6 mg g^{-1} (1-500 mg L^{-1})	39
Magnetite nano particle	5 mg g^{-1} (2–50 ppm)	40
copolymer (PGTDC-COOH)	99.8 mg g^{-1} (25–500 mg L^{-1})	41
Benzoyl thiourea anchored to activated Carbon	82 mg g^{-1} (20-200 mg L^{-1})	42
Rice husk Native SDS-treated Immobilized	 38.9 mg g^{-1} (10-100 mg L^{-1}) 42.4 mg g^{-1} (10-100 mg L^{-1}) 38.0 mg g^{-1} (10-100 mg L^{-1})	Present study